# Physical Behavior of Cross-Linked PEG Hydrogels Photopolymerized within Nanostructured Lyotropic Liquid Crystalline Templates

**Jason D. Clapper and C. Allan Guymon***

*Department of Chemical and Biochemical Engineering, The University of Iowa, Iowa City, Iowa 52242*

*Received September 26, 2006; Revised Manuscript Received December 11, 2006*

ABSTRACT: While hydrogels exhibit numerous characteristics that make them ideal in biological applications, they are typically limited in overall design flexibility due to the rigid dependence of their physical properties and behavior on the chemistry and cross-linking structure of the gel's network. As the demand for hydrogels with precisely engineered properties grows, nanotechnology may provide a means through which to circumvent the inherent drawbacks of hydrogel systems to form unique, highly advanced materials with enhanced properties. In this work, self-assembling nanostructured lyotropic liquid crystalline (LLC) mesophases were used as polymerization templates, directing the formation of highly cross-linked PEGDA hydrogels. A 3-fold increase in both the compressive modulus and diffusive transport is realized in the PEGDA gel as the parent LLC mesophase, and thus the resulting structure of the hydrogel matrix is changed from a low ordered morphology to a system with a high degree of order and geometry. Additionally, the LLC templated hydrogels exhibited unique property relationships, including simultaneous increases in both the water absorptivity and the modulus of the material, behavior that is not observed in nontemplated, traditional PEGDA gels. The results of this study demonstrate that direct control over the physical properties of a cross-linked hydrogel material can be achieved simply by changing the degree of order and geometry imposed on the forming network using nanostructured LLC templates.

## Introduction

Hydrogel research is advancing rapidly as these materials expand in applications ranging from biomaterials to superabsorbents and toxicant removal agents.[1,2] Hydrogels have received particular attention in biomedical applications including contact lenses, biosensors, drug/gene delivery, bioseparations, bioadhesives, and tissue engineering due to their high water content, biocompatibility, high permeability/porosity, and soft tissue characteristics.[3−7] Traditionally, the design principles for controlling the properties of hydrogels have focused on manipulating the network structure of the gel in terms of its cross-linking density, a function of the structure, functionality, and concentration of the monomer in the gel. However, using cross-linking density has limitations as many of the properties of hydrogels are intimately tied to this single parameter. For example, cross-linking density is directly related to hydrogel physical properties such as porosity, water absorptivity, and mechanical strength as well as the behavior of the gel in terms of permeability and diffusive transport.[8−12] Particular to tissue engineering applications, the cross-linking density of the hydrogel has also been linked to the resulting morphology and developing genotype of the encapsulated cells it supports.[13,14] Because of these property relationships, using cross-linking density as a means to optimize a particular property of the gel will inevitably elicit changes, often undesired, in many of the other gel properties, limiting the design flexibility and reducing the relevance of these materials to advanced applications.

To address these issues, researchers have explored alternative methods to control the physical properties of hydrogels, independent of the overall cross-linking density, through the use of topologically restrictive free-moving cross-link junctions,[15] controlled crystalline domains,[16] composite additives,[17] and double-network hydrogels.[18] These studies have achieved various degrees of success in obtaining unique properties in hydrogels previously unattainable using cross-link density as the main design parameter. In addition to the strategies above, the use of nanotechnology is beginning to be explored as a means to engineer the properties of hydrogels for highly advanced biomedical applications.[19] In the past decade, research in nanostructured materials has grown exponentially as nanotechnology continues to alter the ways in which materials are fabricated, synthesized, and processed.[20] By accessing and manipulating the structure of materials on the submicron scale, unique material properties have been observed, including the high strength of carbon nanotubes,[21] property enhancement from nanofillers,[21,22] and biologically attractive nanosurfaces,[23] to name a few.

One of the more promising methods available for the synthesis of materials with nanostructured morphologies is the use of self-assembling media such as lyotropic liquid crystal (LLC) solutions.[24] LLC solutions are distinctive media, possessing both liquidlike fluidity and the long-range order of crystalline solids. Formed by the self-assembly of small molecular weight surfactants in solution, LLCs exhibit a number of highly ordered nanometer scale mesophases that can be controlled by the size, chemistry, and concentration of the surfactant molecules in solution. Their use as polymerization templates, directing the formation of polymer networks into complex architectures, is a particularly promising application of LLCs toward the fabrication of organic nanostructured polymers. To this effect, researchers have focused on the behavior of LLC templated polymerizations with specific regard to the formulation of LLC/monomer blends to generate various mesophases,[25] the polymerization kinetics within these mesophases,[26,27] catalytic enhancement using LLCs as nanoreactors,[28] a platform to compatibilize immiscible monomers,[29] the unique polymeric structures fabricated from LLC templating,[30,31] and the size selectivity of LLC generated membranes.[32]

In addition to the LLC polymerization studies mentioned above, previous research has also documented the effects on

* To whom correspondence should be addressed. E-mail: allan-guymon@uiowa.edu.

10.1021/ma0622377 CCC: $37.00 
Published on Web 01/23/2007

gel properties of templating common lightly cross-linked polymers such as hydroxyethyl methacrylate and acrylamide within LLC mesophases.[33,34] The aim of the present study is to use a more robust, highly cross-linked hydrogel system and perform an in-depth characterization of controlling the physical properties of polymers that is attainable simply by changing the order of the LLC template used to fabricate the gel. Because of the highly dependent nature of physical properties on network structure, it is hypothesized that by manipulating this structure using LLC templates a significant degree of control over the physical behavior of the gel will be realized. For this study, a highly cross-linked PEGDA hydrogel will be polymerized in various LLC mesophases to alter the specific network structure of the resulting hydrogel. Material properties including network swelling, modulus, and diffusive transport will be measured as a function of the type of template used to create each gel. By specifically correlating these three closely related network properties to the parent template used to create each material, a greater understanding of the relationship between the LLC template and final network structure/properties will be obtained. The ability to control the structure of the network, and thus dictate the gel's physical behavior, will prove invaluable as hydrogels are applied to a growing number of diverse and advanced applications.

## Experimental Section

**Materials.** The monomer used in this study was poly(ethylene glycol) diacrylate (PEGDA, Aldrich) with a molecular weight of 575. The surfactant used was polyoxyethylene (10) cetyl ether (Brij 56, Aldrich). 1-Hydroxycyclohexylphenyl ketone (Irgacure 184, Ciba Specialty Chemicals) was used as the photoinitiator. The small release solute used for transport analysis in this study was Chicago Sky Blue Dye (Aldrich) with a molecular weight of 990 and a hydrodynamic radius of ~8 Å as defined as the radii of equivalent spheres of similar molecular weight.[35] All chemicals were used as received with no further purification.

**Preparation of LLC Polymers.** Lyotropic liquid crystalline solutions were synthesized by mixing specific concentrations of monomer, surfactant, deionized water, and photoinitiator. Heat, sonication, and mechanical mixing were employed to obtain homogeneity within the samples and to ease handling of the solutions. In this study, all samples contained 40 wt % monomer, while the surfactant/water ratio was varied to achieve a number of LLC mesophases to serve as polymerization templates. Hydrogels were synthesized by pipetting the LLC/monomer solutions into Teflon molds to make both bar (40 mm × 10 mm × 2 mm) and disk (15 mm diameter, 3 mm height) polymer geometries. The samples were then photopolymerized by placing the mold under a 365 nm UV light source (intensity 1.8 mW/cm$^2$, 10 min) in a nitrogen-purged environment to limit oxygen inhibition. Post polymerization, gels were removed from the mold, solvent exchanged with ethanol to facilitate surfactant removal, and dried in a vacuum oven for 24 h. The average surfactant removal was greater than 95% as determined gravimetrically.

**Characterization of LLC Mesophases.** The optically anisotropic nature of the LLC solutions and photopolymerized gels was characterized using a polarized light microscope (PLM, Nikon Eclipse E600W Pol) equipped with a hot stage (Instec, Boulder, CO). PLM images of various LLC/monomer/water solutions were analyzed for characteristic birefringent light patterns, indicative of the type of order in the liquid crystal solutions. Samples were characterized by placing ~100 $\mu$L between a glass microscope slide and coverslip. Samples were irradiated with a UV source (1.7 mW/cm$^2$, 10 min) to polymerize the solution. Before and after PLM images were compared and used to determine the degree of disruption in the LLC order that occurs during polymerization.

Small-angle X-ray scattering (SAXS) measurements were taken using a Nonius FR590 X-ray apparatus with a standard copper target Rontgen tube radiation source, a camera, a collimation system of the Kratky type, and a PSD 50M position-sensitive linear detector (Hecus M. Braun, Graz). The ratio of the scattering peaks in *d*-spacing was used to determine specific LLC ordered geometry within each sample and, in conjunction with PLM analysis, combined to characterize the concentration-dependent phase behavior of the LLC/monomer formulations both pre- and postpolymerization.

**Network Swelling.** Kinetic water absorption and final equilibrium water absorption were measured gravimetrically by immersing dehydrated hydrogels (post surfactant removal) into 37 °C deionized water and measuring water uptake at given time intervals. Swelling measurements were taken by removing the gel from solution, patting the surface dry, and then recording the mass of the hydrated polymer. Equilibrium water absorption was determined once the mass of a hydrated sample did not change significantly as a function of overall swell time. For swelling and additional tests below, three LLC/polymer bars or disks were made for all sample formulations to obtain a standard deviation for each resulting data point, represented by error bars in the reported figures.

**Network Mechanics.** Dynamic mechanical analysis (DMA, TA Instruments Q800 series) was used to determine the compressive modulus of both dehydrated and swollen samples of the LLC templated hydrogels. Dehydrated disks were used as prepared. For the hydrated modulus tests, dehydrated LLC templated hydrogels were incubated in 37 °C water for 24 h prior to the compressive test. Disk-shaped samples were placed on the compressive clamp of the DMA and compressed to ~90−95% of their original height. Compressive modulus was determined with previously established methods[33] using stress/strain curves from the DMA results.

**Network Transport.** The diffusive behavior of the LLC hydrogels was determined by incorporating a small solute, Chicago Sky Blue dye, into the templated networks of the hydrogel samples. Post polymerization and surfactant removal, dehydrated samples were swollen in a concentrated solution of the dye for ~3 weeks to allow for complete infiltration of the solute within the pores of the hydrogel. Samples were then removed, rinsed, and placed in individual vials of deionized water and incubated at 37 °C. At predetermined intervals, 100 $\mu$L of solution was removed (replaced with 100 $\mu$L of deionized water) from each vial and diluted with 1.9 mL of deionized water in a Spectre cell. The absorbance at 614 nm was determined with a UV−vis spectrometer to determine the concentration of dye released at each time point. Half-life release time constants for each sample were defined as the time required to release half of the remaining dye in the sample, and three consecutive constants were averaged for each templated gel.

Diffusion coefficients for the templated hydrogel materials were determined using a second-order transport equation based on Fickian diffusion.[36] Assumptions included that the dye was evenly distributed within the hydrogel and that the majority of the dye molecules were released from the two large surfaces of the hydrogel bar as opposed to the relatively small side faces due to the thinness of the bar's depth parameter. A subroutine program was used to model the transport equation, generating a number of release profiles for given diffusion coefficients. The generated profiles were then compared to the experimental release profiles of the blue dye to estimate diffusion coefficients for each templated gel.

## Results and Discussion

Numerous reports have focused on methods for incorporating nanotechnology into polymers, often resulting in materials with unique properties ranging from enhanced sieving ability within nanopores[32] to an increase in material strength with additions of nanocomposites.[21,22] In one fabrication method, nanostructured lyotropic liquid crystalline (LLC) mesophases can be used as polymerization templates, imposing a high degree of order on the prepolymerized monomers and thereby structuring the network architecture of the forming polymer. The central aim of this work is not only to use LLCs to create nanostructured

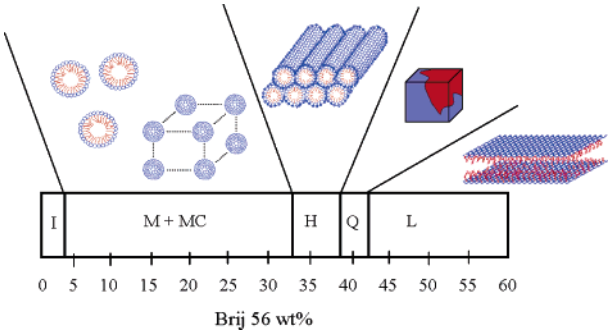


**Figure 1.** Phase diagram for aqueous solutions of 40 wt % PEGDA with increasing concentrations of Brij 56 at 27 °C. Phases are as follows: I = isotropic, M = micellar solution, MC = micellar cubic phase, H = hexagonal phase, Q = bicontinuous cubic phase, and L = lamellar phase.

hydrogels but also to understand the relationships between the LLC template geometry, the network structure of the resulting hydrogel, and the physical behavior of the templated gel.

Because of the strong correlation between physical properties and network structure in hydrogel materials, the hypothesis of the current study is that changes in the hydrogel network structure achieved through LLC templating will have a significant impact on the physical properties of the gel and allow a degree of control over the physical behavior of these materials. To test this hypothesis, three physical properties including swelling, modulus, and permeability have been selected and investigated due to their strong dependence on network structure. These investigations will not only reveal the relationship between LLC template and each of the physical properties generated but also serve to elucidate the overall effect of nanostructure within the matrix of the resulting hydrogel network.

To carry out this study, a highly cross-linked hydrogel material, poly(ethylene glycol) diacrylate (PEGDA), was photopolymerized within a variety of LLC mesophases formed from Brij 56 surfactant and water. As the concentration of Brij 56 surfactant is increased in a 40% PEGDA aqueous solution, a number of LLC phases are formed, including micellar, discontinuous cubic micellar, hexagonal, bicontinuous cubic, and lamellar geometries, providing a spectrum of available polymerization templates. A one-dimensional phase diagram at room temperature is shown in Figure 1 relating the concentration of Brij surfactant to the LLC phase morphology for the LLC/PEGDA systems as determined by PLM and SAXS, along with representations of the corresponding structures of various LLC mesophases. The micellar and cubic micellar mesophases do not exhibit long-range anisotropy and can be considered low order polymerization templates when compared to the higher, long-range order LLC templates such as hexagonal, bicontinuous cubic, and lamellar structures. When comparing the Brij 56/PEGDA/water LLCs to previous reports for the binary system of Brij 56 and water,[37] the progression of phases with surfactant concentration is similar, although the phase transition boundaries are shifted to lower surfactant concentrations. This behavior is due to the presence of PEGDA monomer, which serves to shift the phase boundaries by acting as a cosurfactant in the system.

PEGDA was chosen in this study due to its hydrophilic nature, allowing the monomer to segregate to the aqueous or continuous domains of the LLC mesophase structures. This location within the LLC allows the polymerizing monomer to form a continuous network, reinforcing the surfactant self-assembled structures. A representation of the LLC templating method as well as the

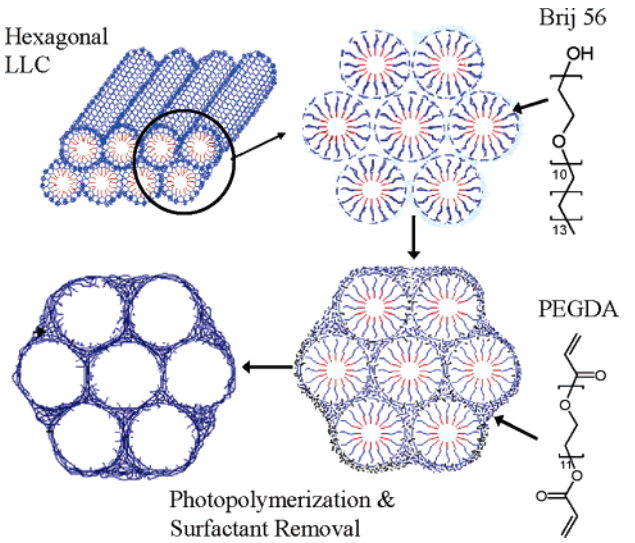


**Figure 2.** Representative LLC templating process, clockwise from upper left: hexagonal LLC mesophase structure, 2D hexagonal LLC with Brij 56 surfactant chemical structure, 2D hexagonal LLC with dispersed PEGDA monomers, and photopolymerized PEGDA in continuous hexagonal arrangement with Brij 56 surfactant removed.

structures of PEGDA and Brij 56 surfactant is shown in the diagram in Figure 2.

**Network Swelling.** The degree of hydrogel network swelling is highly dependent on both the chemical structure of the polymer and matrix parameters such as the cross-linking density of the polymer network. To determine the effects of altering the network structure of templated hydrogels on the degree of swelling in PEGDA materials, samples were polymerized using different LLC templates including micellar, hexagonal, and lamellar mesophases. Figure 3A shows the volumetric swell ($Q$) of templated PEGDA gels as calculated by eq 1 vs time. In eq 1, $M_w$ and $M_d$ are the swollen and dry mass of the gel construct respectively, and $\rho_s$ and $\rho_p$ are the densities of solvent (water) and polymer respectively.

$$Q = \left( \frac{\dfrac{M_w - M_d}{\rho_s}}{\dfrac{M_d}{\rho_p}} \right) + 1 \qquad (1)$$

Networks templated with the higher ordered hexagonal and lamellar LLC morphologies swell rapidly when placed in water with very similar profiles. Alternatively, the low order micellar templated gel exhibits a decreased rate of water uptake as well as a lower equilibrium swell when compared to the higher ordered LLC hydrogels. By removing over 95% of the surfactant from the hydrogels tested in Figure 3A, all samples were both chemically and compositionally similar, implying that the observed differences in water uptake are due to network structural changes, a direct result of the specific template used to create each gel. Interestingly, the geometry of the higher order LLCs (i.e., hexagonal and lamellar) does not seem to influence the rate or overall swelling in these gels to the same degree as the transition from low to higher ordered templates (micellar to hexagonal).

Network swelling in templated hydrogels was further examined by plotting the equilibrium water uptake ($Q_e$) for PEGDA hydrogels with increasing surfactant concentration to produce the spectrum of LLC phases. In Figure 3B, the equilibrium water swell in the templated hydrogel samples is shown as a function

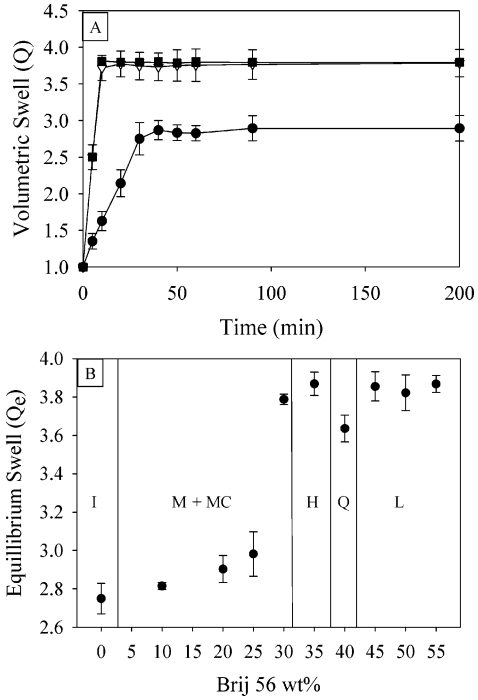


**Figure 3.** (A) Swelling profiles of 40 wt % PEGDA (MW 575) templated with 50 wt % Brij 56 (lamellar) (▼), 35 wt % Brij 56 (hexagonal) (■), and 10 wt % Brij 56 (micellar) (●). (B) Equilibrium volumetric swell of 40 wt % PEGDA templated with increasing amounts of Brij 56 surfactant to create specific polymer templates. I = isotropic, M = micellar, MC = micellar cubic phase, H = hexagonal phase, Q = bicontinuous cubic phase, and L = lamellar.

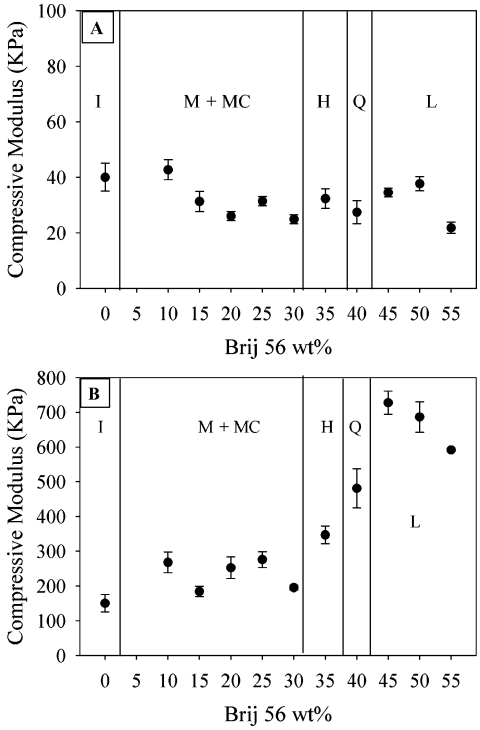


**Figure 4.** Compressive modulus of (A) hydrated and (B) dehydrated PEGDA (40 wt %) hydrogels templated with increasing amounts of Brij 56 surfactant to create specific polymer templates. I = isotropic, M = micellar solution, MC = micellar cubic phase, H = hexagonal phase, Q = bicontinuous cubic phase, and L = lamellar.

of the concentration of surfactant and template geometry used to make each material. The phase diagram for the prepolymerized PEGDA/LLC systems is included with the plot of equilibrium water swell in Figure 3B to illustrate the effect of the specific LLC template structure on the physical properties of the hydrogel. A slight increase in swelling is observed as surfactant concentration is increased from 5 to 25 wt %. However, as the Brij 56 concentration is increased near the first phase boundary, marking the transition to a higher ordered hexagonal LLC template geometry, a significant increase in swelling is observed. Though the main variance in network swelling appears to be due to the transition from lower ordered templates to higher ordered LLCs, small geometric changes within the higher ordered LLC templates (i.e., hexagonal to bicontinuous cubic) also show a repeatable, statistically significant change in overall swell with this particular LLC template system.

**Mechanical Experiments.** In addition to altering the rate and overall water swell of templated polymers, it has been shown in previous research that the template geometry will have a significant effect on the mechanical properties of a templated polymer system as well.[33] To gain a more in-depth look at the effects of prepolymerization monomer order on the macromechanical properties of the structured PEGDA, compressive tests were performed on the PEGDA hydrogels templated with increasing concentrations of Brij 56. Figure 4A shows the resulting compressive modulus of the swollen gels as a function of the surfactant concentration and the template morphology used to create each hydrogel. This figure indicates that as surfactant concentration and thus overall order in the monomer solution are increased, no general trend in the compressive modulus of the swollen hydrogels is observed. This is surprising given the fact that the samples templated with the higher order LLC mesophases (>30% Brij 56) swell ~100% more than their lower order templated counterparts. It has been well documented that an increase in the overall water uptake in a hydrogel to this degree is typically accompanied by a significant drop in modulus.[9,38]

To further investigate this anomaly, a separate set of disks templated with the same surfactant concentrations used in Figure 4A were generated. Instead of allowing these disks to reach equilibrium swell, they were not rehydrated after fabrication and surfactant removal. As shown in Figure 4B, a significant increase in the compressive modulus of the dehydrated materials templated with higher ordered LLCs is seen when compared with the isotropic lower order templates. Again, all samples tested in Figure 4B are compositionally and chemically identical, with only the template that was used to polymerize each as the sole contributor to the variation shown in physical properties between the materials. The use of higher order LLC templates elicits a 3-fold increase in modulus over the low order templates, an observation that is most likely attributed to the highly uniform structure and induced orientation of cross-linked PEG in the LLC templated gels that combine to effectively resist the compressive forces on the material.

As stated above, an increase in the amount of water in a hydrogel material will serve to decrease the compressive modulus of the system, a trend that is evident when comparing the 10% Brij samples in both the hydrated and dehydrated state (Figure 4, A and B, respectively). However, focusing on the hydrated compressive modulus in Figure 4A, as the LLC template in the monomer formulation is altered and swelling is increased (Figure 3B), there is no statistical change in the modulus of these gels. This deviation from typical hydrogel behavior is attributed to the counteracting effects of both an increase in the modulus of the gels (Figure 4B) and the increased degree of swelling in these materials (Figure 3B) as the polymerization template is transitioned from a low order solution

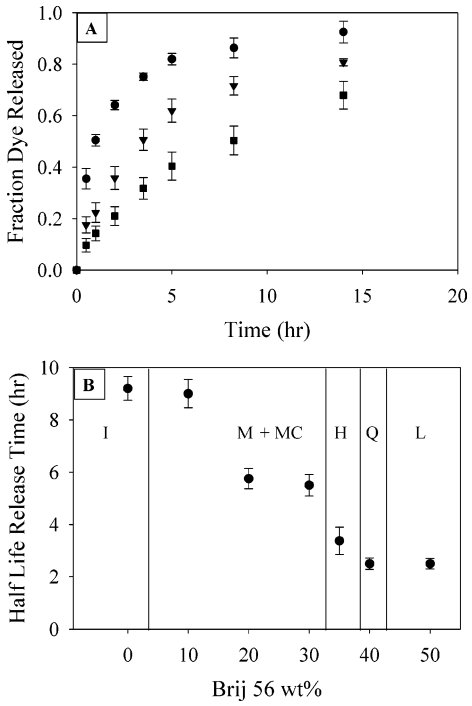


**Figure 5.** (A) Release profiles of Chicago Sky Blue dye from 40 wt % PEGDA templated with 50 wt % Brij 56 (lamellar) (●), 20 wt % Brij 56 (cubic micellar) (▼), and 0 wt % Brij 56 (isotropic) (■). (B) Release time required for approximately half of the remaining dye in 40 wt % PEGDA samples with increasing concentrations of Brij 56 surfactant to create specific polymer templates. I = isotropic, M = micellar solution, MC = micellar cubic phase, H = hexagonal phase, Q = cubic phase, and L = lamellar.

to a higher order LLC. The increase in water uptake with LLC templating decreases the strength of the gel and, in this case, serves to effectively counteract the increasing dry modulus in this material, resulting in little net overall change in the compressive modulus of the hydrated LLC networks.

**Diffusion Experiments.** With the strong relationship between the physical properties (i.e., swelling and dehydrated modulus) and the LLC template used to fabricate each material, it is reasonable to assume that the nanostructured morphology of the LLC template used has a significant impact on the resulting hydrogel network architecture that is at the core of the macrophysical properties evaluated. Furthermore, it is also expected that a level of control over the matrix morphology in the LLC hydrogels would also directly affect the transport behavior of the hydrogel networks. To investigate the influence of LLC templating on the diffusive transport behavior of structured PEGDA hydrogels, a small blue dye solute was incorporated into LLC/PEGDA hydrogels templated with varying LLC morphology. The fraction of dye released for three different network structures (lamellar, cubic, and micellar) as a function of time is shown in Figure 5A. It was found that the higher order LLC lamellar template, having the greatest degree of swelling (Figure 3B), also demonstrates the most rapid release of the dye when compared to the lower ordered templates.

Diffusive transport in the LLC templated PEGDA was further analyzed by plotting the half-life release time for networks templated with increasing concentration of Brij 56 surfactant to generate the spectrum of LLC phases. It is observed in Figure 5B that small variations in the template geometry elicit step changes in the release rate of the dye, with decreasing half-life time as the template is changed from micellar, to discontinuous cubic, hexagonal, bicontinuous cubic, and lamellar LLC phases. In this figure, more rapid diffusion is represented by smaller half-life times defined as the time required to release ~50% of the dye in each network. Therefore, a general trend is observed in which the PEGDA hydrogels templated with the higher order LLCs exhibit much faster diffusion times for the dye solute than do the low order templated gels. This trend can be attributed to both the greater degree of swelling in these samples and the long-range continuous geometric void spaces generated by the higher order LLCs (hexagonal, bicontinuous, lamellar). In contrast, the low order micellar and cubic micellar templates swell to a lesser degree and form gels with discontinuous voids that require the releasing dye to travel a more tortuous path.

Diffusive behavior in hydrogels has been closely linked with the cross-linking density and water uptake of the gel as network swelling has previously been reported to "open up" the network, increasing pore size and increasing the rate of solute diffusion through the network.[11] Although a greater degree of swelling in the higher order LLC templated PEGDA networks may be a contributing factor to the advanced release rate for these gels, analysis of key samples in Figure 5 further serves to deconvolute the effects of increased swell and specific architecture of the network on the transport behavior of the material. For example, the large increase in diffusion rate between the cubic micellar (30% Brij 56) and lamellar (50% Brij 56), two samples that swell to the same degree, suggests that network structural differences contribute significantly to the variations in diffusive behavior between these two samples.

To further investigate the effects of LLC structure on the diffusive behavior of the templated PEGDA hydrogels, a model was employed to describe the relationship between diffusivity and network structure in these materials. A great deal of previous research has been devoted to the development of mathematical models to describe the physical properties of hydrogels, including water absorptivity, modulus, porosity, and permeability, through their relation to network structural parameters such as cross-linking density.[12,35,38,39] Because of its specific application to PEG hydrogels, a free-volume diffusion model[35] (eq 2) was chosen to model the LLC templated PEGDA gels.

$$\frac{D_g}{D_0} = \left(1 - \frac{r_s}{\xi}\right) \exp\left(-\left(\frac{\nu_2}{1-\nu_2}\right)\right) \qquad (2)$$

In eq 2, $D_g$ is the solute diffusivity within the swollen hydrogel, $D_0$ is the solute diffusivity in the swelling solvent calculated using the Stokes−Einstein equation, $r_s$ is the hydrodynamic radius of the solute, $\xi$ is the mesh size of the hydrogel network (a function of cross-linking density), and $\upsilon_2$ is the percent volume of polymer in the swollen hydrogel (inverse of $Q$ in eq 1). Using this model, predicted diffusion coefficients $D_g$ were calculated for each of the templated PEGDA hydrogels using the degree of swelling found experimentally for each gel (Figure 3). As expected, the more swollen gels created using the higher order LLC templates yielded slightly higher predicted diffusion coefficients than the low order templates due to the increased pore size in these gels. The predicted diffusion coefficients for the LLC templated PEGDA hydrogels are listed in Table 1 and shown in Figure 6.

To compare the predicted diffusion coefficients generated by the free-volume model to the experimental results generated through dye release experiments, a diffusion-controlled transport equation for a one-dimensional, uniformly loaded film[36] was modeled to generate a range of release curves with provided diffusion coefficients. By matching these generated curves with the experimental release profiles of blue dye solute from the templated PEGDA hydrogels (Figure 5A), the experimental

**Table 1. Diffusion Coefficients for LLC Templated PEGDA Hydrogels[a]**

| | | *D* | |
|---|---|---|---|
| wt % Brij 56 (template) | swell ($Q_e$)/$v_2$ | free vol model | exptl |
| 0 (isotropic | 2.75/0.364 | 7.72 ± 0.12 | 8.3 ± 1.4 |
| 10 (micellar) | 2.82/0.355 | 8.02 ± 0.08 | 8.3 ± 1.4 |
| 20 (cubic micellar) | 2.90/0.345 | 8.41 ± 0.31 | 16.7 ± 1.4 |
| 30 (cubic micellar) | 3.79/0.264 | 11.59 ± 0.09 | 19.4 ± 2.8 |
| 35 (hexagonal) | 3.87/0.258 | 11.86 ± 0.22 | 38.9 ± 2.8 |
| 40 (bicontinuous cubic) | 3.64/0.275 | 11.11 ± 0.30 | 44.4 ± 2.8 |
| 50 (lamellar) | 3.87/0.258 | 11.86 ± 0.14 | 44.4 ± 2.8 |

[a] Diffusion coefficients (*D*, $10^8$ cm$^2$ s$^{-1}$) found experimentally and as predicted from the free volume diffusion model, of Chicago Sky Blue dye at 37 °C as it is released from the templated cross-linked PEGDA samples. The template phase used to create each PEGDA network, the resulting equilibrium swell ($Q_e$), and polymer volume fraction ($v_2$) are included.

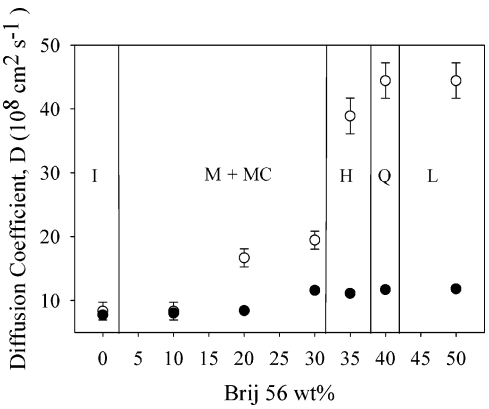


**Figure 6.** Experimental (○) and model predicted (●) diffusion coefficients, *D* ($10^8$ cm$^2$ s$^{-1}$), of Chicago Sky Blue dye at 37 °C as it is released from templated PEGDA materials. The template phase used to create each PEGDA network is included.

diffusion coefficient for each LLC templated hydrogel could be estimated. The diffusion coefficients for the LLC templated hydrogels are listed in Table 1 and shown in Figure 6. The hydrogels generated with low order templates exhibited diffusive behavior similar to what is predicted by the free-volume model given the degree of network swell with these gels. Although small changes in network structure are expected due to the micelle and cubic micellar features of the LLC template used to create each gel, these structures are discontinuous, and the bulk of the network will be relatively similar to the random morphology hydrogel networks for which the free volume model was designed.

Contrary to the agreement between model and experimental diffusion coefficients determined for the low order templated gels, experimental diffusion coefficients for the higher order LLC templated gels (Figure 6) are much greater than what is predicted by the diffusion model. Although the model predicts a slight increase in diffusion over the lower order templated gels due to an increased degree of swelling, it is unable to predict the observed diffusion rate in the higher order templated materials. Further insight can be gained by looking at the model and the matrix structure that is expected from the higher order LLC templates. The free-volume diffusivity model is specifically designed to relate network structural parameters of a swollen hydrogel to diffusive behavior given that the network in question is of random morphology with an average cross-link density and pore size indicative of the entire network. However, this is not the case with the higher order LLC templated gels as a templated structure in these networks would possess both relatively small pores in the polymer-rich regions as well as fairly large pores formed from the continuous structures of the LLC surfactant template. The swelling of the hydrogel networks, on which the free volume diffusivity model is based, is directly related to the overall network cross-linking density or average pore size in the gel. The presence of LLC structures shift this pore size average leading to a minor increase in water uptake that is translated into the small increase in diffusivity predicted by the model. In reality, the release of solute from the LLC PEGDA networks will follow the large, long-range pores formed from the higher order LLC templates, which in turn will have a dramatic effect on diffusive transport, limiting the accuracy of the free volume diffusivity model that is based primarily on the degree of hydrogel swelling. In fact, to achieve the same diffusivity observed for the higher order LLC templated gels, a random morphology PEG hydrogel would have to swell to ~12 times greater than what was actually recorded for the hexagonal, cubic, and lamellar LLC gels.

The discrepancy between the diffusion coefficients found for the LLC templated gels and the degree of swelling in these gels suggest that the LLC pore size and the overall cross-linking density of the network are relatively independent, a theme that is evident in the earlier reported physical property data in this study. For example, increases in swelling and diffusion rates that are typically associated with major modifications to the cross-linking density of the gel were achieved with little collateral effect on the swollen mechanical properties of the network, a parameter that is also closely linked to the overall cross-linking density of the material. Furthermore, an increase in the compressive modulus of the dehydrated templated PEGDA gels, typically associated with an increase in cross-linking density and decrease in swell and permeability, is instead accompanied by an increase in swelling and diffusivity in these same gels. These conflicting relationships suggest that the LLC directed pores are able to alter select physical properties of the PEGDA hydrogels without greatly affecting the overall cross-linking density of the network as well as other physical properties directly related to this parameter.

One of the main themes of this work is that the nanostructured LLC templates are controlling the structure of the PEGDA hydrogel networks, and in turn, the structure of each hydrogel network is directly responsible for the physical behavior of that gel. Thus, simply by changing the LLC template used, the physical properties of the polymerized hydrogels can be precisely controlled. Furthermore, the nontraditional property relationships that are observed throughout this study, including the high transport and mechanical strength of the templated hydrogels, are also directly attributed to the unique, highly ordered geometries imposed on the resulting hydrogel networks through the LLC templating process.

Recent studies have demonstrated that the type of surfactant used, the monomer size, monomer functionality, and the polymerization kinetics all play a significant role in the LLC templating process, yielding materials that span the spectrum from polymer structures that are grossly phase separated from the liquid crystal to network structures that are clearly a copy of the parent LLC template.[31,40−42] Recent work has also demonstrated that phase separation, occurring as the growing molecular weight polymer chains separate from the highly organized LLC mesophase, can be significantly reduced using high-speed initiation techniques such as photopolymerization in an effort to "trap" the LLC structure within the forming cross-linked network.[40] To examine the LLC templating process for the PEGDA/Brij56 formulations in this work, PLM and SAXS characterization techniques were performed both before and after the polymerization of each system to determine the extent of

LLC disruption that occurs during the reaction. In general, the optical anisotropy and scattering peak ratios characteristic of the particular nanostructure in the system do not change during photopolymerization, indicating that the order and the geometry of the LLC monomer solutions are retained to a great degree in the polymerized network. Furthermore, the results obtained in this study in which chemically and compositionally equal hydrogels exhibit vastly different physical behavior due to LLC templating also suggest that the resulting hydrogel structure is significantly influenced by the order and geometry of the LLC template. Finally, the structure of the parent template and hydrogel can be used to control and obtain unique physical properties in the templated hydrogels.

## Conclusions

Nanostructured LLC mesophases were used as polymerization templates, imposing a high degree of order and geometry on the structure of a cross-linked PEGDA hydrogel system in an effort to influence the physical properties of the gel. It was found that simply by changing the geometry of the parent LLC template, and thus the architecture of the forming hydrogel network, significant property enhancements were achieved. When compared to the nontemplated gels, a 100% increase in water uptake, a 3-fold increase in mechanical strength, and a 3-fold increase in diffusive transport were observed in the PEGDA material as the network of the hydrogel was templated with highly ordered, nanostructured LLCs. Additionally, the LLC templated hydrogels exhibited unique property relationships, including simultaneous increases in both the water absorptivity, permeability, and the modulus of the material, behavior that is not typically observed in nontemplated PEGDA gels. The knowledge and control gained from manipulating the relationships between the nanostructured architecture of the parent LLC templates, the structure of the hydrogel networks, and their resulting physical properties allow for the fabrication of enhanced hydrogel materials that will play a significant role in a growing number of advanced applications.

**Acknowledgment.** The authors gratefully acknowledge financial support from The University of Iowa through a Biosciences Initiative Grant and Presidential Fellowship and from The National Science Foundation (PECASE CTS-0626395).

## References and Notes

(1) Buchholtz, F. L.; Peppas, N. A. *Superabsorbent Polymers: Science and Technology*; American Chemical Society: Washington, DC, 1994.
(2) Bajpai, S. K.; Johnson, S. *React. Funct. Polym.* **2005**, *62*, 271−283.
(3) Yasuda, H. *Macromol. Biosci.* **2006**, *6*, 121−138.
(4) Hahn, M. S.; Taite, L. J.; Moon, J. J.; Rowland, M. C.; Ruffino, K. A.; West, J. L. *Biomaterials* **2006**, *27*, 2519−2524.
(5) Jeong, B.; Bae, Y. H.; Lee, D. S.; Kim, S. W. *Nature (London)* **1997**, *388*, 860−862.
(6) Drury, J. L.; Mooney, D. J. *Biomaterials* **2003**, *24*, 4337−4351.
(7) Andreopoulos, F. M.; Persaud, I. *Biomaterials* **2006**, *27*, 2468−2476.
(8) Maleki, A.; Kjoniksen, A. L.; Knudsen, K. D.; Nystrom, B. *Polym. Int.* **2006**, *55*, 365−374.
(9) Perera, D. I.; Shanks, R. A. *Polym. Int.* **1996**, *39*, 121−127.
(10) Gibson, S. L.; Jones, R. L.; Washburn, N. R.; Horkay, F. *Macromolecules* **2005**, *38*, 2897−2902.
(11) Scott, R. A.; Peppas, N. A. *Biomaterials* **1999**, *20*, 1371−1380.
(12) Lu, S.; Anseth, K. S. *Macromolecules* **2000**, *33*, 2509−2515.
(13) Bryant, S. J.; Anseth, K. S.; Lee, D. A.; Bader, D. L. *J. Orthop. Res.* **2004**, *22*, 1143−1149.
(14) Kim, B. S.; Mooney, D. J. *Trends Biotechnol.* **1998**, *16*, 224−230.
(15) Okumura, Y.; Ito, K. *Adv. Mater.* **2001**, *13*, 485−487.
(16) DeLong, N. S.; Agrawal, S. K.; Bhatia, S. R.; Tew, G. N. *Macromolecules* **2006**, *39*, 1308−1310.
(17) Haraguchi, K.; Takehisa, T. *Adv. Mater.* **2002**, *14*, 1120−1124.
(18) Gong, J. P.; Katsuyama, Y.; Kurokawa, T.; Osada, Y. *Adv. Mater.* **2003**, *15*, 1155−1158.
(19) Peppas, N. A.; Hilt, J. Z.; Khademhosseini, A.; Langer, R. *Adv. Mater.* **2006**, *18*, 1345−1360.
(20) Rosei, F. *J. Phys.: Condens. Matter* **2004**, *16*, S1373−S1436.
(21) Kueseng, K.; Jacob, K. I. *Eur. Polym. J.* **2006**, 220−227.
(22) Decker, C.; Keller, L.; Zahouily, K.; Benfarhi, S. *Polymer* **2005**, *46*, 6640−6648.
(23) Kay, S.; Thapa, A.; Haberstroh, K. M.; Webster, T. J. *Tissue Eng.* **2002**, *8*, 753−761.
(24) Hentze, H. P.; Kaler, E. W. *Curr. Opin. Colloid Interface Sci.* **2003**, *8*, 164−178.
(25) Pawlowski, D.; Tieke, B. *Langmuir* **2003**, *19*, 6498.
(26) DePierro, M. A.; Olson, A. J.; Guymon, C. A. *Polymer* **2005**, *46*, 335−345.
(27) Lester, C. L.; Smith, S. M.; Jarrett, W. L.; Guymon, C. A. *Langmuir* **2003**, *19*, 9466−9472.
(28) Gin, D. L.; Weiqiang, G. U.; Pindzola, B. A.; Zhou, W. J. *Acc. Chem. Res.* **2001**, *34*, 973−980.
(29) Clapper, J. D.; Guymon, C. A. *Adv. Mater.* **2006**, *18*, 1575−1580.
(30) Jan, L. S.; Radiman, S.; Siddig, M. A.; Muniandy, S. V.; Hamid, M. A.; Jamali, H. D. *Colloids Surf., A* **2004**, *251*, 43−52.
(31) Wadekar, M. N.; Pasricha, R.; Gaikwad, A. B.; Kumaraswamy, G. *Chem. Mater.* **2005**, *17*, 2460−2465.
(32) Zhou, M.; Kidd, T. J.; Noble, R. D.; Gin, D. L. *Adv. Mater.* **2005**, *17*, 1850−1853.
(33) Lester, C. L.; Smith, S. M.; Colson, C. D.; Guymon, C. A. *Chem. Mater.* **2003**, *15*, 3376−3384.
(34) McCormick, D. T.; Stovall, K. D.; Guymon, C. A. *Macromolecules* **2003**, *36*, 6549−6558.
(35) Lustig, S. R.; Peppas, N. A. *J. Appl. Polym. Sci.* **1988**, *36*, 735−747.
(36) Crank, J. *The Mathematics of Diffusion*; Clarendon Press: Oxford, 1975.
(37) Coleman, N. R. B.; Attard, G. S. *Microporous Mesoporous Mater.* **2001**, *44*, 73−80.
(38) Flory, J. *Principles of Polymer Chemistry*; Cornell University: Ithaca, NY, 1953.
(39) Brannon-Peppas, L.; Peppas, N. A. *Chem. Eng. Sci.* **1991**, *46*, 715.
(40) DePierro, M. A.; Carpenter, K. G.; Guymon, C. A. *Chem. Mater.* **2006**, *18*, 5609−5617.
(41) Antonietti, M.; Caruso, R. A.; Goltner, C. G.; Weissenberger, M. C. *Macromolecules* **1999**, *32*, 1383−1389.
(42) Anderson, D. M.; Strom, P. *Physica A* **1991**, *176*, 151−167.

MA0622377